PROCEEDINGS, Eighteenth Workshop on Geothermal Reservoir Engineering
Stanford University, Stanford, California, January 26-28, 1993
SGP-TR-145

INTERFERENCE TEST ANALYSIS AT THE TAKIGAMI GEOTHERMAL FIELD, JAPAN

Ryuichi ITOI(1), Michihiro FUKUDA(1), Kenji JINNO(2) and Hiroki Gotoh(3)

(1)Geothermal Research Center, Kyushu University, Kasuga, JAPAN 816
(2)Faculty of Engineering, Kyushu University, Fukuoka, JAPAN 812
(3)Idemitsu Geothermal Co. Ltd, Chiyodaku, Tokyo, JAPAN 100

ABSTRACT

A long term interference test was conducted under conditions of multiwell variable flow rate at Takigami for about ten months in 1987. The test data have been analyzed with an on-line analysis method on the basis of the line-source solution. This method employs Kalman filtering to process the data and then provides the best estimates of reservoir transmissivity and storativity when a new pressure data at an observation well becomes available. The pressure changes measured at seven observation wells have been analyzed with the present method using an infinite reservoir model. The data from one observation well have been further analyzed assuming a presence of a linear boundary. Performances of the parameters estimated for different reservoir models are compared. Fairly good estimates of reservoir parameters are obtained on the basis of an infinite reservoir model for two wells using the entire pressure data whereas for other five wells using a part of the pressure data.

INTRODUCTION

Pressure interference tests have advantages in providing information on average values of reservoir parameters such as transmissivity(T) and storativity(S) in the area where observation and active wells are located(Leaver et al., 1988; Gotoh, 1990). Computer assisted methods to analyze the test data are powerful tools for reservoir engineers. This is because that conventional methods of type curve matching have some difficulties in processing actual situations such as multiple active wells varying their flow rate with time. Two computer codes have been developed on the basis of the line-source solution derived under assumptions of homogeneous, isotropic, and porous type of reservoir (McEdwards and Benson, 1981;Arellano et al., 1990). This solution is superposed both in time and space to meet the situation above and the presence of hydrologic boundary by introducing image well(s). These codes have employed the nonlinear least squares method for parameter determination, because the solution is nonlinear with respect to the reservoir parameters. These programs, however, store all the pressure data at an observation well during computation, requiring a large memory on a computer. Furthermore, poor initial guesses of the parameters may lead to the failure in determining good estimates.

In order to cope these problems, particularly for the analysis using personal computers, we have developed methods to analyze interference test data using Kalman filtering(Itoi et al., 1990; Itoi et al., 1992). On the assumption of a series of pressure data measured at an observation well, these methods yield best estimates of unknown parameters at every moment when a new pressure value becomes available. In this paper, we have analyzed the interference test data at the Takigami geothermal field with the method which is an expansion of the Sen's work (Sen,1984;Itoi et al., 1992). The results indicate that the estimated transmissivity from seven observation wells varies in the range from 1.04×10^{-7} to 8.91×10^{-7} $m^3/Pa \cdot s$.

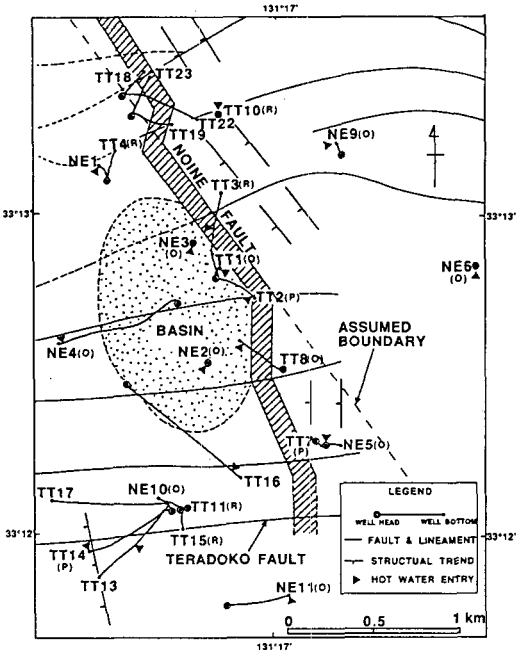

Fig.1 Location map of wells at the Takigami geothermal field. Signs of (P) denote the production well, (R) the reinjection well, and (O) the observation well during the interference test(modified after Hayashi et al., 1988)

INTERFERENCE TEST AT TAKIGAMI

The Takigami geothermal field is located in the Beppu-Shimabara graben in Kyushu Island, Japan. This field has been under exploration for power generation since 1979, and a power plant of installed capacity 25 MW is expected starting its operation in 1996. The interference test in 1987 was conducted with three production wells which discharged enough fluids to generate 26 MW of electricity. The fluid production had been continued for about six months, and the separated water was reinjected through five

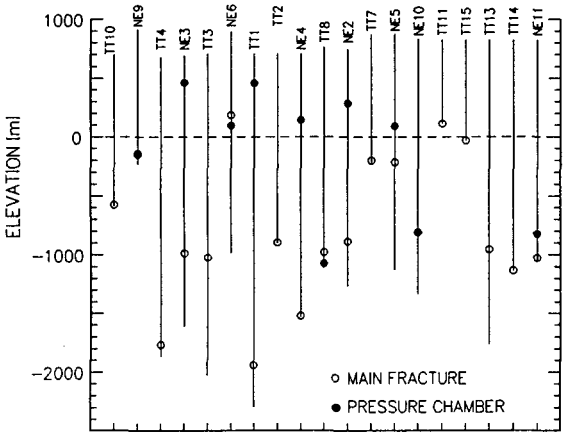

Fig.2 Depths of well, main fracture(open circle), and pressure chamber(solid circle).

reinjection wells(Hayashi et al., 1988). The pressure changes caused by operating these wells had been monitored at seventeen wells including these active wells with pressure measurement apparatus of capillary tube type. Seven out of ten observation wells presented apparent pressure response during the test.

Fig. 1 shows the location map of wells and geological features at Takigami. The reservoir is of water dominated type, and is divided into two areas by the Noine fault running NNW to SSE as shown in Fig.1. High temperature zone at about 250 °C has been found in the south-western part of the field and lower temperature zone in the north-eastern part(Hayashi et al.,1988). Therefore, a reservoir management will be designed to separate production and reinjection zones horizontally by 1 to 2 km to avoid the inflow of reinjected water into the production zone. Fig.2 shows the depths of main fracture or main water loss zone, indicated by the open circle, of the wells which were used during the test in 1987. The solid circle represents the installed depths of pressure chamber for downhole pressure measurement at the observation wells.

Figs.3(a) and (b) show the flow rate history of production and reinjection wells, respectively. Flow rate of production wells was kept almost constant during the test except TT14 ranging its flow rate 200 -270 m^3/h. On the other hand, all reinjection wells show highly variable flow rates with time. Both production and reinjection wells were stopped their operation by about 2.8×10^5 min since the start of the test. Very good communication between the two reinjection wells, TT11 and TT15, was confirmed, thus their flow rates are added and presented as a single flow rate shown in Fig.3(b).

ANALYSIS METHOD OF INTERFERENCE TEST

Pressure response at an observation well caused by producing or reinjecting fluids at a constant flow rate at an active well can be expressed by the line-source solution on the basis of isotropic, homogeneous, and infinite porous type of reservoir. The effects of multiple active wells and their flow rate change with time on the pressure response can be expressed by superposing the line-source solution

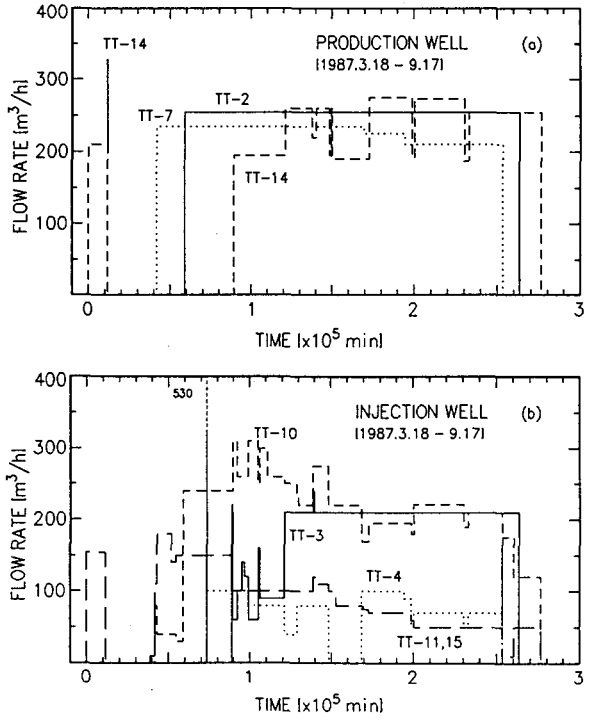

Fig.3 Flow rate history of (a)production wells and (b) reinjection wells.

both in time and space. Moreover, the variable flow rates can be processed by dividing these into a series of linear segments of flow(McEdwards and Benson, 1981). Thus, pressure change at an observation well at time t_k (k=1,2, •, •) can be expressed as

$$\Delta p(t_k) = \frac{1}{4\pi T} \sum_{n=1}^{N} \left(\sum_{j=1}^{J} C_{n,j} \right) \qquad (1)$$

where $\Delta p(t_k)$ is the pressure change at the observation well at time t_k, T is the transmissivity(=kh/μ, k:permeability, h:reservoir thickness, μ:viscosity of fluid). N is the total number of active wells, j is the number of flow segments, and J is the total number of flow segments prior to the time t_k. $C_{n,j}$ is expressed as follows

for $1 \le j \le J-1$

$$C_{n,j} = \left[A_{n,j} + B_{n,j}(t_k - \tau_{n,j})(1 + u_{n,j}) \right] \left[Ei(-u_{n,j+1}) - Ei(-u_{n,j}) \right]$$

$$- B_{n,j} \left[(t_k - \tau_{n,j}) exp(-u_{n,j}) - (t_k - \tau_{n,j+1}) exp(-u_{n,j+1}) \right] \qquad (2)$$

for $j = J$

$$C_{n,j} = \left[A_{n,j} + B_{n,j}(t_k - \tau_{n,j})(1 + u_{n,j}) \right] \left[-Ei(-u_{n,j}) \right]$$

$$- B_{n,j} \left[(t_k - \tau_{n,j}) exp(-u_{n,j}) \right] \qquad (3)$$

and $u_{n,j}$ and u_{nj+1} are

$$u_{n,j}=\frac{Sr_n^2}{4T(t_k-\tau_{n,j})} \quad (4) \qquad u_{n,j+1}=\frac{Sr_n^2}{4T(t_k-\tau_{n,j+1})} \quad (5)$$

where $A_{n,j}$ is the flow rate of j-th segment of n-th active well at time t_k, $B_{n,j}$ is the inclination of this flow segment, $\tau_{n,j}$, $\tau_{n,j+1}$ are the time when j-th flow segment of n-th active well begins and ends, respectively. $Ei(-u)$ is the exponential function of u, S is the storativity(=ϕch, ϕ: porosity, c:compressibility), and r_n is the radial distance between n-th active well and the observation well.

A presence of a hydrologic boundary in the test area can be modelled by assuming it as a linear vertical boundary. The effects of the presence of the linear boundary on pressure behavior at the observation well can be generated by locating image well(s) at a symmetric position across the boundary(Matthews and Russell, 1967; Sageev, et al., 1985). To simplify the subsequent notation , we denote the time t_k by expressing variables with subscript k. Therefore, the pressure response in the presence of the linear boundary is given

$$\Delta p_k = \Delta p_{aw} \pm \Delta p_{im} \quad (6)$$

where Δp_{aw} represents the pressure change caused by operating active wells and Δp_{im} by image wells. Positive sign is for the impermeable boundary and negative one for the constant pressure boundary. Further formulation is developed on the basis of Eq.(1) for the simplicity.

Eq.(1) represents a relation between the measured pressure change at an observation well and the reservoir parameters, T and S, to be estimated, thus this equation corresponds to the measurement equation to form Kalman filtering. This relation, however, is apparently nonlinear with respect to the reservoir parameters. Thus, this equation should be linealized to form Kalman filtering. For this purpose, we have adopted and modified Sen's technique(Sen, 1984) in which he analyzed a pumping well test to estimate aquifer parameters using Kalman filtering under conditions of constant flow rate from a single pumping well. In order to form the observation equation, an additional formula defining u_k is introduced

$$u_k = \sum_{n=1}^{N} u_{n,J} = \frac{S}{T}\sum_{n=1}^{N}\frac{r_n^2}{4(t_k-\tau_J)} \quad (7)$$

Taking logarithms of both side of Eqs.(1) and (7), and by rearranging, we obtain

$$\log \Delta p_k - \log\left[\frac{1}{4\pi}\sum_{n=1}^{N}\left(\sum_{j=1}^{J} C_{n,j}\right)\right] = -\log T \quad (8)$$

$$\log u_k - \log\left[\sum_{n=1}^{N}\frac{r_n^2}{4(t_k-\tau_J)}\right] = -\log T + \log S \quad (9)$$

Writing the left side of the equations as y_1 and y_2 leads to the observation equation in a vector form:

$$\mathbf{y}_k = H_k\mathbf{x}_k + \mathbf{v}_k \quad (10)$$

where $\mathbf{y}_k = [y_1, y_2]^T$ $\mathbf{x}_k = [\log T, \log S]^T$

H_k is the observation matrix and is time invariant as

$$H_k = \begin{bmatrix} -1 & 0 \\ -1 & 1 \end{bmatrix} \quad (11)$$

$[\,]^T$ indicates transposition. Eq.(10) is apparently a linear function of $\mathbf{x}$ whose components are logarithms of T and S. The reservoir parameters, T and S, can be assumed to be constant during the test, and hence the state equation can be written

$$\mathbf{x}_{k+1} = \mathbf{x}_k + \mathbf{w}_k \quad (12)$$

where $\mathbf{v}_k$ and $\mathbf{w}_k$ are the measurement and state noises assumed to be zero-mean, mutually uncorrelated, white noise of covariance matrices V_k and W_k, respectively.
On the basis of the reservoir system described by Eqs.(10) and (12), the algorithm of Kalman filtering provides the best estimate of state vector at time t_k when a new measurement becomes available. By denoting the best estimate at t_k as $\hat{\mathbf{x}}_{k/k}$ where the "hat" indicates estimate, this will be given by updating the previous estimate, $\hat{\mathbf{x}}_{k/k-1}$, as follows

$$\hat{\mathbf{x}}_{k/k} = \hat{\mathbf{x}}_{k/k-1} + K_k(\mathbf{y}_k - H_k\hat{\mathbf{x}}_{k/k-1}) \quad (13)$$

where K_k is the Kalman gain matrix and is given as

$$K_k = P_{k/k-1}H_k^T\left[H_kP_{k/k-1}H_k^T + V_k\right]^{-1} \quad (14)$$

Superscript -1 denotes inversion. The error covariance matrix associated with the present estimate is expressed as

$$P_{k/k} = P_{k/k-1} - K_kH_kP_{k/k-1} \quad (15)$$

For estimating process at the next time step, the state vector is predicted by

$$\hat{\mathbf{x}}_{k+1/k} = \hat{\mathbf{x}}_{k/k} \quad (16)$$

and the error covariance matrix is given as

$$P_{k+1/k} = P_{k/k} + W_k \quad (17)$$

Calculations of parameter estimating can be started by giving initial values for P and $\mathbf{x}$. The components of the observation vector expressed by the left-hand sides of Eqs.(8) and (9) can not be calculated even when a new pressure value at time t_k becomes available, because these components include the parameters to be estimated. Hence these values are substituted by the prior estimates: $\mathbf{x}_{k/k-1}$ (Sen, 1984). This substitution may introduce false information into the components of the observed vector when the poor initial guesses of parameters are given. As a result, the method fails to determine the good estimates at each time step. To overcome this deficiency, we repeat a whole calculation process in which parameters are estimated using pressure data from beginning to end of the measurement. Here, we define the last estimates of parameters determined at a time when the last pressure

value is measured. Then, these final estimates obtained during the present iteration are given as the initial guesses for the next iteration process. Calculations are iterated until the differences between the newly obtained final estimates and the previous ones to satisfy a given convergence criterion. Fig.4 shows a flow chart for the calculation of parameter estimation above.

ANALYSIS OF INTERFERENCE DATA

The pressure data from seven observation wells(NE2, NE3, NE4, NE5, NE10, NE11, TT1) have been analyzed with the method in the preceding section on the basis of an infinite reservoir model. The data from NE11 have been further analyzed by assuming a presence of a linear boundary indicated by the dotted line in Fig.1.

The pressure data were recorded at an interval of six hours, and the total number of data collected for one observation well reached up to 1200 at maximum during the test. The data were, then, processed to extract one from every 10 pressure values and to remove faulty values apparently caused by malfunctioning of the measurement apparatus. The present method has been demonstrated that a convergence of estimation may be guaranteed as far as the ratio of initial guesses of T and S (S/T) being given to be one or less(Itoi et al., 1992). Thus, all calculations are started by giving initial values of $T=1\times10^{-5}$ m^3/Ps•s and $S=1\times10^{-5}$ m/Pa. In addition, initial values of diagonal and nondiagonal components of matrix P are given as 100 and 0, respectively. Covariance matrices of the measurement and the state noises are set to be constant as 0.01 and 0 for diagonal and nondiagonal parts.

In the following, the analyses of the data from NE11 are described in detail on the basis of an infinite reservoir model and of a model in the presence of a linear boundary. NE11 is a deviated well and located southern most part of Takigami as shown in Fig.1. Main water loss zone of this well seems to be on southward extension of the Noine fault. A careful examination of the measured pressure data of NE11 and the flow rate history of active wells seems to support the effects of interference by active wells TT14, and TT7 which is located eastern side of the Noine fault. Therefore, we have analyzed the pressure data by assigning the flow rates of these two active wells. The number of the pressure data used is 75. The data are first analyzed on the basis of an infinite reservoir model. Convergence of calculations is attained after four iterations of estimating process, and the final estimates obtained are $T=2.41\times10^{-7}$ m^3/Pa•s and $S=1.78\times10^{-7}$ m/Pa.

The present method provides estimates at each time step when a new pressure value becomes available, thus the estimated values of T and S are used to predict the pressure value at the next time step, $p_{k+1/k}$, which is compared with the measured value, p_{k+1}. Fig. 5(a) shows a comparison between the two kinds of pressure values during the fourth iteration process. The circle represents the measured pressure and the solid line the predicted one. The predicted pressure values show a fairly good match with the measured ones throughout the test period except in the later times when the pressure recovery starts. During this period, small discrepancies between the two kinds of pressures are recognized. The result implies that the estimated values at the present time are good enough to achieve nearly perfect prediction of the pressure value at the next time. Fig.5(b) shows the performances of estimated values of parameters

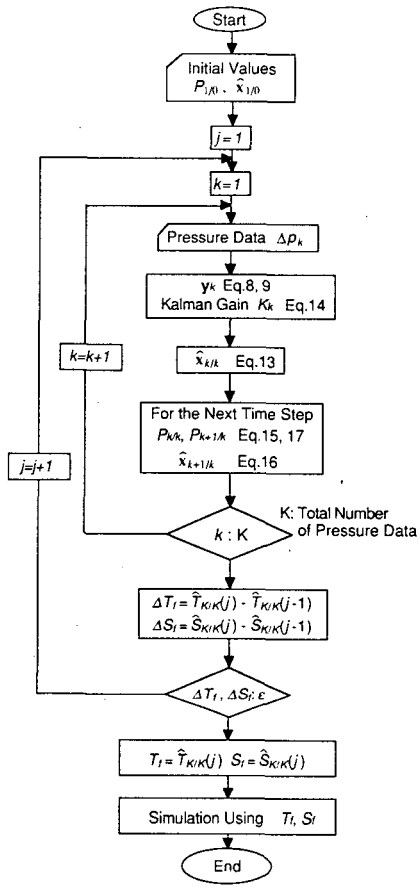

Fig.4 Flow chart for parameter estimation using Kalman filtering.

at each time step during the fourth iteration process. The circle represents the estimated transmissivity(T) and the triangle the estimated storativity(S). Small variations in both estimates can be seen in the early times of the data. This variation may be attributed to the flow rate history of TT14 which stopped and resumed discharging and that of TT7 which started discharging during this period as shown in Fig.3(a). Then, the estimates show gradual increases followed by stabilized values up to about 2.5×10^5 min. In turn, they exhibit continuous decreases as approaching the end of the measurement. The final estimates obtained are $T=2.41\times10^{-7}$ m^3/Pa•s and $S=1.78\times10^{-7}$ m/Pa. The pressure response was simulated using these final estimates, and the result is compared with the measured pressure values in Fig.5(c). Good matches are observed only for short periods in the very early and later times. The simulated pressure departs markedly with time from the measured ones up to 2.5×10^5 min. Then, the discrepancies between the two kinds of pressures become small as it approaches the end of the measurement. This poor match is attributed to the final estimates of T and S used for simulating the entire pressure data are lower than the estimates at the middle times. However, major features of the measured values such as sharp drop at about 0.4×10^5 min and start of pressure recovery when fluids production stopped are successfully reproduced.

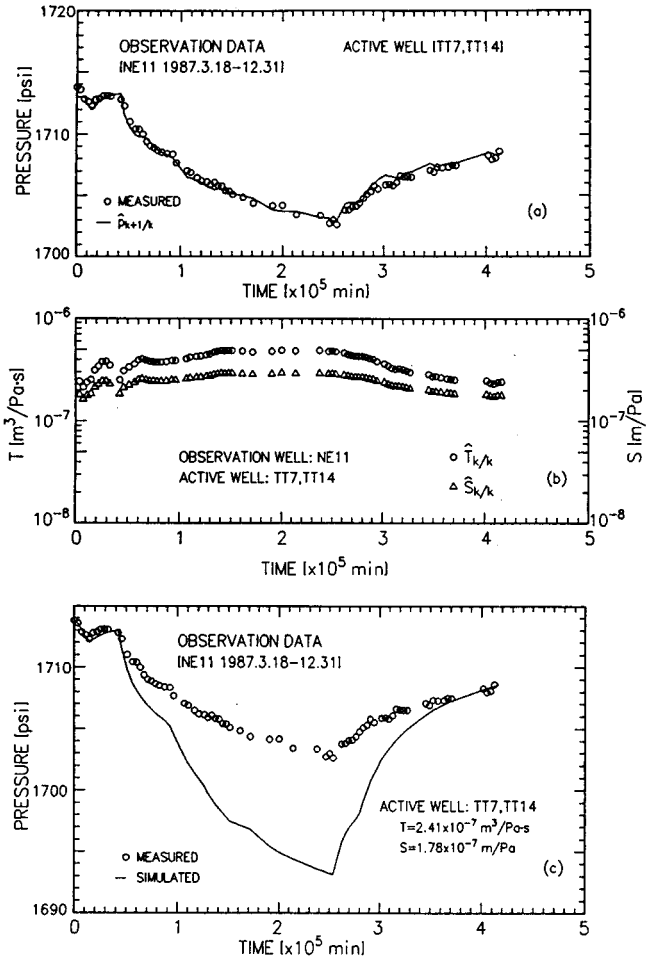

Fig.5 Results of analysis of the pressure data from NE11, (a)predicted pressure(solid line) compared with measured one during the fourth iteration process of parameter estimating, (b) performance of estimated transmissivity(T) and storativity(S) with time, (c) comparison of simulated pressure values using the final estimates of T and S with measured ones.

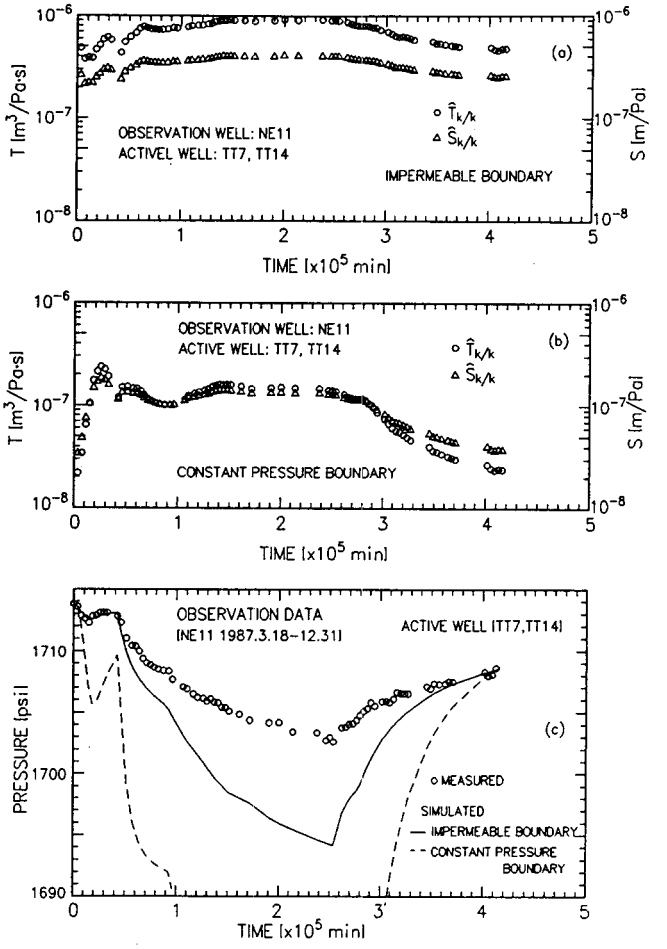

Fig.6 Results of analysis in a presence of a linear boundary for NE11, (a)performance of estimated transmissivity(T) and storativity(S) with time for the case of impermeable boundary, (b) for the case of constant pressure boundary, (c) comparison of simulated pressure values using the final estimates of T and S determined for the cases above.

Next, we have analyzed the data of NE11 with an infinite reservoir model in the presence of the linear boundary located as shown in Fig.1. NE11 is apparently received interference from both production wells of TT14 and TT7, and thus it may be reasonable to assume the presence of the boundary on the eastern side of TT7 if existed. Two kinds of linear boundaries, impermeable and constant pressure, are considered during the analysis. Figs.6(a) and (b) show performances of estimated parameter values of T and S for the cases of impermeable boundary(IB) and of constant pressure boundary(CPB), respectively. The result for the case of IB shows similar performance to that of the infinite reservoir case in Fig.5(b), but both estimates show larger values in comparison with those in Fig.5(b) throughout the test period. On the other hand, the case of CPB shows rapid rise in both estimates at the beginning followed by fairly stabilized values during the middle times. Decrease rates of estimates in the later times are, however, much larger compared with the case of IB. The final estimates attained are 1) T=4.75x10^{-7} m^3/Pa·s and S=2.55x10^{-7} m/Pa for the IB case, 2)2.40x10^{-8} m^3/Pa·s and 3.74x10^{-8} m/Pa for the CPB case. Both values of estimated transmissivity and storativity of the IB case are larger than those of the CPB case by an order of magnitude. These parameter values are used for simulating the pressure

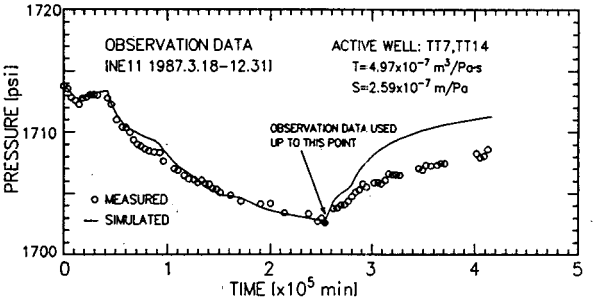

Fig.7 Comparison of simulated pressure values using the final estimates of T and S with measured ones for NE11.

response for each reservoir model, and the results are compared with measured data in Fig. 6(c). Discrepancies between the measured and the simulated values for the case of IB are similar to the result of an infinite reservoir model as shown in Fig.5(c). On the other hand, discrepancies between the two kinds of pressures for the CPB case are much larger than those for the IB case, implying that a constant pressure boundary is not likely to present at this part of the area. Therefore, these results suggest that no models could fully express the entire pressure data of NE11.

A careful examination of the estimation behaviors of T and S in Fig. 5(b) suggests that monotonous decreases in the estimates in the later times may be affected by faulty data since the preceding estimates remain relatively stable. The faulty data may be attributed to the measurement error caused by mulfunctioning of the apparatus. Another possible reason is the fact that the real system do not satisfy the reservoir models used during the analysis. Therefore, calculations for parameter estimation are repeated using the pressure data from the beginning up to 2.54×10^5 min, indicated by the solid circle in Fig.7. Final estimates obtained after five iterations of calculations are $T=4.97 \times 10^{-7}$ $m^3/Pa \cdot s$ and $S=2.59 \times 10^{-7}$ m/Pa. Simulated pressure values using these estimates are compared with measured ones in Fig. 7. The solid line representing the simulated pressure shows a satisfactory match to the measured pressure until the time indicated by the solid circle. The simulated values, however, gradually depart from the measured ones with time. This result indicates that the early half of the data can be fully expressed using an infinite reservoir model.

Analyses of the pressure data from other observation wells also provide fairly good estimates if only a part of the pressure data is used except NE4 and NE10 for which entire pressure data are used. The results of the estimated values are summarized in Table.1. The estimated transmissivity varies in the range 1.04×10^{-7} - 8.91×10^{-7} $m^3/Pa \cdot s$ and the storativity in the range 2.62×10^{-8} - 1.34×10^{-6} m/Pa. Estimated storativity of NE5 shows large value of 3.79×10^{-3} m/Pa which may be physically unrealistic. These transmissivities give kh values in the range from 11.7 to 100.6 darcy•m when the viscosity of water at 240 °C is employed.

Table 1 Estimated transmissivity(T) and storativity(S) on the basis of an infinite reservoir model.

Observation Well	Active Well	Estimates	
		T ($m^3/Pa \cdot s$)	S (m/Pa)
NE2	TT2, TT7, TT14	4.60×10^{-7}	1.34×10^{-6}
NE3	TT3, TT14	2.24×10^{-7}	2.62×10^{-8}
NE4	TT14	1.04×10^{-7}	1.07×10^{-7}
NE5	TT7	2.68×10^{-7}	3.79×10^{-3}
NE10	TT14	1.23×10^{-7}	8.74×10^{-8}
NE11	TT7, TT14	4.97×10^{-7}	2.59×10^{-7}
TT1	TT2, TT14	8.91×10^{-7}	2.08×10^{-7}

CONCLUSIONS

1) Interference test analysis using Kalman filtering provides good estimates of transmissivity(T) and storativity(S) at each moment when a new pressure value at an observation well is measured.

2)Simulated pressure changes using the final estimates of T and S do not always show a satisfactory match to the entire pressure data even the estimates at every moment are good.

3)A careful examination of performances of estimated T and S with time may provide information on the effects of using inadequate reservoir model during the analysis or the faulty data caused by mulfunctioning of measurement apparatus.

4) Estimated permeability-thickness product(kh) from the analyses of seven observation wells varies in the range 11.7 to 100.6 darcy•m.

REFERENCES

Arellano, V.M., Iglesias, E.R., Arellano, J. and Perez, M.R.(1990) ANAPPRES V3.0: Automatic Interference-Test Analysis in Personal Computers, *GRC Trans.*, Vol.14, PartII, 1271-1278.

Gotoh, H.(1990) Reinjection Plan for the Takigami Geothermal Field Oita Prefecture, Japan, *GRC Trans.*, Vol.14, Part II, 897–899.

Hayashi, J., Motomatsu, T. and Kondo, M.(1988) Geothermal Resources in the Takigami Geothermal Area, Kyushu, Japan., *Chinetsu*, Vol.25, No.2, 1–27(in Japanese with English abstract).

Itoi, R., Arakawa, H., Fukuda, M. and Jinno, K.(1990) The Application of Kalman Filter to Pressure Interference Test Analysis, *GRC Trans.*, Vol.14, Part II, 1207– 1210.

Itoi, R., Fukuda, M., Jinno, K. and Gotoh, H.(1992) Interference Test Analysis Method Using the Kalman Filtering and Its Application to the Takigami Geothermal Field, JAPAN, *GRC Trans.*, Vol.16, 657– 662.

Leaver, J.D., Grader, A. and Ramey Jr., H.J.(1998) Multiple-Well Interference Testing in the Ohaaki Geothermal Field, *SPE FE*, Vol.3, No.2, 429-437.

Matthews, C.S. and Russell, D.G.(1967) Pressure Buildup and Flow Tests in Wells, *Monograph Series*, SPE of AIME

McEdwards, D.G. and Benson, S.M.(1981) User's Manual for ANALYZE – – A Variable- Rate, Multiple-Well, Least Squares Matching Routine for Well-Test Analysis, *LBL*-10907.

Sageev, A., Horne, R.N. and Ramey Jr., H.J.(1985) Detection of Linear Boundaries by Drawdown Tests:A Semilog Type Curve Matching Approach, *Water Resources Research*, Vol.21, No.3, 305-310.

Sen, Z.(1984) Adaptive Pumping Test Analysis, *J. of Hydrology*, Vol.74, 259-270.